ISSN 1855-9913

Journal of the Laser and Health Academy
Vol. 2021, No.1; www.laserandhealth.com

Smooth Resurfacing by Hyper Stacking of Er:YAG Laser Pulses; a Histological and Clinical Study

Adrian Gaspar[1], Marcelo Tettamanti[2], Branka Korošec[3], Matjaž Lukač[4]
1Espacio Gaspar Clinic, Mendoza, Argentina;
2Biotechnolaser, 19 NE Lofting Way, Stuart, FL 34994, USA;
3Fotona, d.o.o., Stegne 7, Ljubljana, Slovenia;
4Institut Jozef Stefan, Jamova 39, Ljubljana, Slovenia.

ABSTRACT

Non-ablative Er:YAG laser "smooth-resurfacing" of skin and mucosa has attracted significant attention in recent years due to the technique's safety and excellent clinical results. The goal of this study was to histologically determine which smooth-resurfacing protocol is the most effective for skin regeneration, and to evaluate the contribution to the overall tissue regeneration process of the intense heat-shock biomodulation resulting from superficial heat-shock triggering.

The results of the study are consistent with previous reports indicating that Er:YAG laser smooth-resurfacing possesses a unique non-ablative regenerative characteristic, whereas the standard deep-thermal coagulation is accompanied and enhanced by the additional intense heat-shock biomodulation process.

When comparing different smooth-resurfacing protocols, the obtained immuno-histological data indicates that the most effective protocol is the HyperStack™ protocol based on hyper stacking of Er:YAG laser pulses, resulting in synergistic activation of both mechanisms, the superficial heat-shock triggering and the deep-tissue coagulation mechanisms.

The tissue regeneration process was observed to persist for more than 3 months following HyperStack™ smooth-resurfacing, with the total amount of positive fibroblasts located within skin depths of up to 1600 μm doubling at the 21-day follow up and increasing by four times at the 3-month follow up. Following HyperStack™ treatment of abdominal skin, the waist circumference was measured to decrease by 2 cm at 21 days, 5 cm at 3 months and 6 cm at 5 months.

Finally, based on the results of the study, a range of recommended HyperStack™ parameters is provided for treatments using the T-Runner robotic scanner.

Key words: Er:YAG, V-SMOOTH, resurfacing, smooth-resurfacing, heat shock triggering, variable heat shock, T-Runner scanner.

Article: J. LA&HA, Vol. 2022, No.1; onlineFirst.
Received: January 10, 2022; Accepted: April 20, 2022

I. INTRODUCTION

Patients and physicians look for less invasive techniques to prevent or reverse signs of aging. For many years ablative lasers have been used successfully for the treatment of wrinkles, but their use is limited by the associated pain and down time, and by the relatively high risk of side effects and complications. Therefore, the demand for non-ablative techniques that are minimally invasive yet effective is growing fast.

a) Smooth-resurfacing

Non-ablative "smooth-resurfacing" of the skin and mucosa has in recent years attracted significant attention due to the technique's safety and excellent clinical results [1-15]. Laser treatments with Fotona SMOOTH® mode Er:YAG energy have been determined to initiate changes in the cutaneous and mucosal tissues without causing unwanted direct epithelial ablation. Through activation of the tissue healing response, fibroblasts are activated to migrate to the treated tissue volume, where they initiate the production of extracellular matrix and tissue remodeling [1]. Fotona SMOOTH® mode Er:YAG lasers have been, for example, very successfully used for Fotona4D® face-lifting [10-11] and skin tightening [2, 3].

The smooth-resurfacing consists of delivering an Er:YAG laser pulse sequence to the treated soft tissue (see Fig. 1), consisting of a controlled number (N) of laser pulses of very short duration (0.3 - 0.6 ms), with cumulative fluences (Fs) below the ablation threshold. During earlier, more aggressive non-ablative treatments, cumulative fluences close to or slightly above the ablation threshold were used [16-21]. On the other hand, with smooth-resurfacing the cumulative fluence is not only bellow the ablation threshold, but

also below the heat pain tolerance threshold. This self-protecting feature of smooth-resurfacing results in the extreme safety of this technique.

In spite of the technique's "smoothness" the regenerative response of the tissue to smooth-resurfacing is significant. This is because during an Er:YAG laser pulse sequence, the laser-generated heat dynamics exhibit two phenomena (see Fig. 1): i) a slow gradual build-up of the spatial temperature distribution over the total duration of the sequence, extending several hundred microns deep into the tissue (see Fig. 1), with the long-duration surface temperatures (T_s) typically below 50-70°C; as well as ii) intense short-duration thermal pulses resulting from individual laser pulses i, with peak temperatures (T_{max-i}) above 80°C at the surface, leading to intense heat-shock biomodulation leading to a regeneration of deeper-lying tissues [22]. The Fotona SMOOTH® treatment thus represents a unique combination of the actions of two regenerative mechanisms involving both a short-exposure and a long-exposure biochemical process.

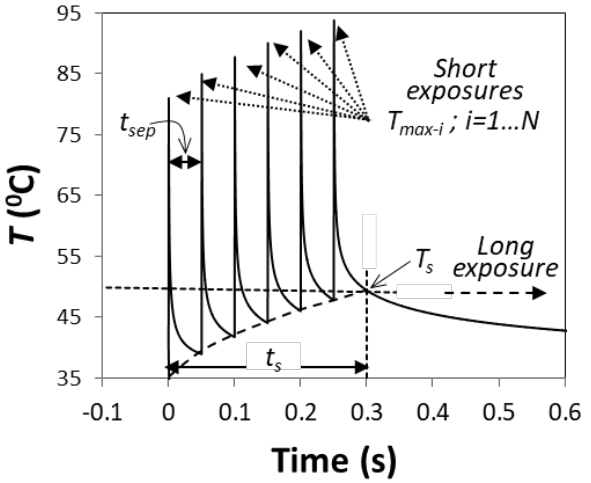

Fig. 1: Er:YAG laser's smooth-resurfacing pulse sequence (example for N = 6 is shown) and resulting temperatures. Due to the fast thermal diffusion from the heated ≈ 1-3 μm thin superficial tissue layer, the duration of the thermal exposure (texp) to high temperature peaks Tmax-i is extremely short (texp < 1 ms). The temperature Ts is the final sequence temperature, representing the long-duration temperature exposure.

b) Robotic T-Runner for skin tightening

For skin tightening, a special T-Runner™ robotic scanner has been introduced that automatically distributes high repetition rate Er:YAG laser pulses with individual laser spot size (d) over a larger skin treatment area, ensuring that each treatment spot experiences irradiation by a large number of pulses at an appropriately reduced repetition rate [2]. The T-Runner thus enables an overall area treatment speed at the laser's maximal output power capability while intelligently preventing any undesired local superficial temperature build-up. Using this technology, it is possible to distribute the delivered energy over a large number of low-fluence pulses, as required for superficial triggering and deep skin coagulation, without the need for local or general anesthesia.

The T-Runner robotic scanner operates in a variable V-Smooth mode that consists of six micro pulses within the adjustable macro pulse duration (125-625 ms). By selecting the V-Smooth duration, fluence, and total number of delivered V-Smooth pulses, the T-Runner technology enables the practitioner to control the effect of the performed smooth-resurfacing to be either predominantly superficially triggering at one extreme, predominantly deep coagulative at the other extreme, or a combination of both mechanisms in-between.

The goal of our study was to determine which of the above three main protocol choices is most effective for skin regeneration, and to evaluate the contribution of the superficial heat-shock triggering to the over-all tissue regeneration process. The results of the different smooth-resurfacing protocols were evaluated histologically and clinically.

II. MATERIALS AND METHODS

a) Laser

The laser used was an SP Dynamis Er:YAG (λ = 2940 nm) laser system equipped with the T-Runner® robotic scanner (both manufactured by Fotona, d.o.o.). The T-Runner robotic scanner operated in a variable Fotona SMOOTH® (V-Smooth™) mode that delivers V-Smooth™ macro pulses consisting of six consecutive, equally spaced micro pulses i, within adjustable macro pulse durations of V-Smooth = 125, 250, 375, 500 or 625 ms. A larger number of micro pulses can be delivered by stacking several (N_{stack}) V-Smooth macro pulses. The resulting over-all number of delivered micro pulses is N = 6 x Nstack, with the irradiation duration (t_s) equal to ts = V-Smooth x N_{stack}. The over-all delivered Er:YAG laser fluence (in J/ cm²) was equal to $F_s = N \times F_p$, where F_p is the single micro-pulse fluence.

The T-Runner robotic scanner is equipped with two separate distance holders, resulting in two scan area sizes ("Face" and "Body"), optimized for treating either smaller (single scan area: ≈ 4 x 4 cm²) or larger (single scan area: ≈ 8 x 8 cm²) body areas. The choice of the distance holder also determines the corresponding individual laser spot size (d = 7 mm for "Face" or d = 9 mm for "Body").

STP heat pain and coagulation depth indicator. Based on the results of a detailed heat pain threshold

study [24], and smooth-resurfacing numerical model calculations [2, 3, 22, 24], the Dynamis laser system software includes an advanced intelligent algorithm for determining the STP (Surface Temperature Parameter) value and the coagulation depth z_c that are automatically calculated and displayed on the user interface, depending on the selected V-SMOOTH mode parameters. The STP varies with the selected laser parameters and is dependent on the patient's sensitivity in the range of STP ≤ 85-110% for parameters resulting in a pain threshold temperature in the range of $T_s \approx$ 45-50°C for treatments without anesthesia. Similarly, the STP value is in the range of STP ≈ 110% -140% ($T_s \approx$ 50-53°C) for treatments below the pain threshold when topical anesthesia is used. While the pain threshold varies from patient to patient, the STP feature provides the practitioner with initial information about whether the selected combination of parameters is within the safe and comfortable range.

b) Protocol analysis

An analysis was performed in order to pre-select clinical protocols to be tested. We applied: i) a numerical model of the physical process of tissue resurfacing, with the details of the physical model and parameters used described in [2, 23, 24]; and ii) an Arrhenius damage integral-based VHS (Variable Heat Shock) chemical model of the tissue response to the short-duration and long-duration thermal exposures, as described in [2, 3, 22, 24].

According to the VHS model, the critical temperature for irreversible tissue damage represents a combined effect of two limiting Arrhenius' processes (See Fig. 2), defining cell viability at extremely long and short exposure times, t_{exp} [22].

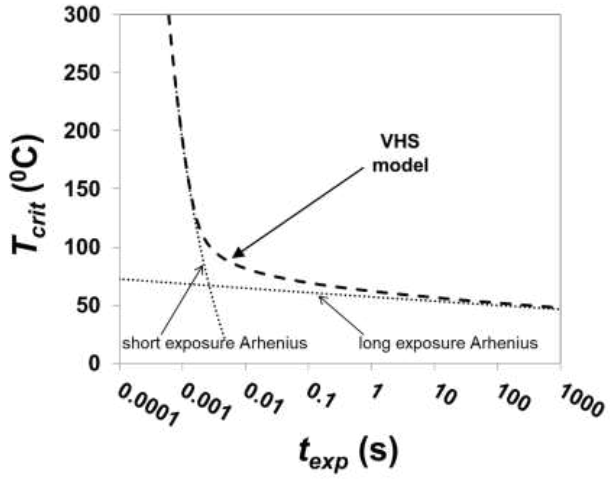

Fig. 2: VHS (Variable Heat Shock) model of tissue response [22]. For very short thermal exposures the critical temperature is significantly higher than what would be expected from a single Arrhenius' dependence determined for thermal exposures longer than about 1 second.

The analysis of the level of superficial triggering (A_{trig}), and of the deep-tissue response represented by the coagulation depth (z_c) was made for treatments at the patient's pain tolerance threshold for two smooth-resurfacing conditions: without and with topical anesthesia.

Amplitude of short-exposure superficial triggering. As can be seen from Fig. 2, for extremely short duration thermal exposures (t_{exp} < 1 ms), such as encountered during exposures to high temperature peaks $T_{max\text{-}i}$ during Er:YAG smooth-resurfacing (see Fig. 1), the critical temperature is above the soft tissue's threshold temperature of 256°C required for Er:YAG laser ablation [22]. This means that despite their intensity, the high temperature peaks $T_{max\text{-}i}$ (see Fig. 1) are not expected to cause irreversible damage. Instead, they result in heat-shock generated biomodulation, representing an additional, indirect mechanism of action for regenerating epithelial and deeper-lying connective tissues [1, 22, 25-29], which is complementary to the conventional direct slow stimulation of fibroblasts [30]. The superficial heat-shocking resembles the micro-needling technique, aimed at stimulating tissue renewal through triggering cell-to-cell communication and wound-healing like response, without inducing epidermal injury through removal or ablation [31, 32]. The smooth-resurfacing laser-induced heat-shock biomodulation mechanism can thus be viewed as non-ablative thermal "needling" (i.e., triggering) of the total treated skin surface, with the action of the spatially sharp needles being replaced by the action of temporarily "sharp" but spatially extended heat-shock pulses.

The amplitude of superficial heat-shock triggering was evaluated by assuming that the level of thermal "needling" is related to the superficial damage resulting from the short-duration exposures, the probability Pi of thermal damage caused by each pulse, i = 1…N, calculated from

$$P_i = 1 - \exp(-\Omega_i), \quad (1)$$

where the tissue damage response Ω_i was calculated using a standard Arrhenius rate equation [33-36].

The probability-summation model [37, 38] was used to calculate the cumulative short-exposure Arrhenius process damage to the superficial tissue layer, following a series of i = 1…N, intense short-duration thermal exposures to $T_{max\text{-}i}$.

$$P_{superf} = 1 - (1 - P_1)(1 - P_2) \ldots (1 - P_N), \quad (2)$$

and the superficial tissue response Ω_{superf} was then

obtained using Eq. 1, with P_i and Ω_i replaced by P_{superf} and Ω_{superf}.

It is to be noted here that although generally there is a cumulative effect in multiple-pulse exposures [39], the cumulative mechanism may vary depending on the type of tissue and irradiation [38, 39]. This means that, the short-exposure tissue response Ω_{superf} as calculated using the probability-summation model should be taken merely as an indication of the actual amplitude (A_{trig}) of heat-shock triggering ($A_{trig} \approx \Omega_{superf}$), and not as the absolute superficial tissue damage.

Long-exposure deep-tissue coagulation. The deep-tissue damage integral Ω_{deep} resulting from the long-duration temperature extending deeper into the tissue (see Fig. 3) is characterized predominantly by the long-pulse exposure process. It was calculated by integrating the damage over temperature instead of over time, using the algorithm developed for calculating tissue damage for temporally non-square-shaped thermal exposure pulses [2, 3, 22, 24]. The coagulation depth zc was obtained as the tissue depth below which the calculated cell injury Ω_{deep} was smaller than 0.5.

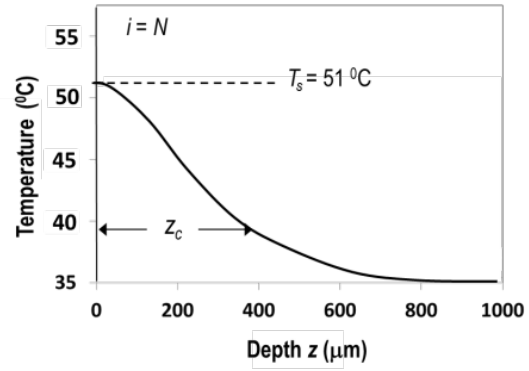

Fig. 3: Example of the spatial temperature profile extending deep into the tissue by the end of a pulse sequence (i = N; t = t_s).

c) Treatment protocol

Altogether, 15 healthy volunteers were included in the clinical study. A signed informed consent was obtained, and the procedure was performed according to the Declaration of Helsinki. Volunteers were treated in four weekly sessions using different treatment protocols on the abdomen or neck.

The protocol analysis revealed three distinct treatment regimens for smooth-resurfacing:

Intense smooth-resurfacing protocol for maximal superficial heat-shock triggering (with resulting high heat-shock triggering amplitude and shallow coagulation depth);

Deep hyper-stacking smooth-resurfacing protocol for maximally deep thermal stimulation (with low heat-shock triggering amplitude and deep coagulation depth); and

HyperStack™ smooth-resurfacing protocol consisting of hyper stacking of laser pulses for combined superficial triggering and deep-thermal stimulation within a single procedure (with medium values of heat-shock triggering amplitude and coagulation depth).

In the initial stage of the study, the abdomens of three female patients were treated using topical anesthesia, with each patient treated with one of the three basic smooth-resurfacing clinical protocols as selected based on the protocol analysis (see Table 1). The Er:YAG laser treatment fluences Fs in these protocols were adjusted to result in the highest possible below-pain threshold value of STP = 110% - 140% for smooth-resurfacing under topical anesthesia.

The topical anesthesia was applied 20 minutes prior to a treatment, and consisted of Benzocaine 15%, Lidocaine 15% and Procaine 15% in a water preparation.

Table 1: Three types of clinical protocols (Intense, Deep hyper-stacking HyperStack) used in the study.

T-Runner Body with topical anesthesia	Protocol	INTENSE	DEEP HYPER	HYPER
V-SMOOTH mode	ms	625	625	625
Fluence F_s	J/cm²	4.2	14	11
N_{stack}	/	2	20	11
STP	%	111	137	140
Coagulation depth z_c	μm	111	780	522
HEAT shock trig. A_{trig}.	/	0.98	0.054	0.24

Based on the initial results that showed the HyperStack™ protocol to result in the largest pro-collagen expression, the next stage of the study focused on the HyperStack™ protocol only. Histological results were for one of the patients followed at 21 days and 3 months following the treatment.

d) Histology and imunohistochemistry

In five of the patients, punch biopsies were taken under local anesthesia using injectable 2% lidocaine to evaluate the tissue damage as well as tissue improvement. Biopsies were embedded in formalin and paraffin. For a general view of the tissue, structural organization sections were stained with hematoxylin/eosin.

Masson's trichrome and immunohistochemistry using antibodies against pro-collagen type I (TaKaRa, Bio Europe S.A., Gennevillier, France) were used for more detailed examination [19]. The activation of "positive" fibroblasts was observed by staining antibodies that were generated against active collagen type I - producing fibroblasts. Microscopic observation was performed with a standard optic microscope (Primo Star, Carl Zeiss, Germany) with magnifications of 4X, 10X, 40X, and 100X. The clinical-histological correlation was performed to determine the pro-collagen formation.

e) Measurement of skin shrinkage

Waist circumference. Since tightening of abdominal skin displaces the umbilical level line, the bones (that do not displace) were used for reference (See Fig. 4).

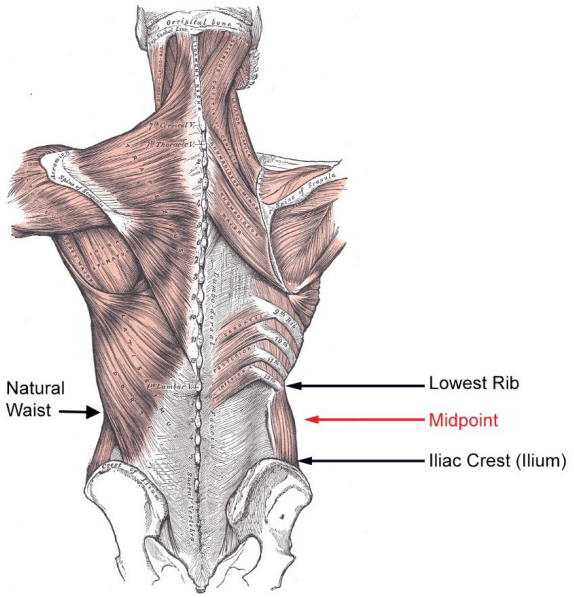

Fig. 4: Landmarks used for measuring waist circumference. *Image: Gray H. Anatomy of the Human Body. (1918). FIG. 409.*

The patient was asked to stand upright, and the distance between the iliac crest and the lower rib was measured on both sides. A white pencil dot was placed right at the midpoint of each flank.

The waist circumference was measured with a cloth metric ruler around the waist in the midpoint line, established by the two white reference points (see Fig. 5). Measurement of the waist circumference was made after asking the patient to exhale completely and hold their breath for several seconds.

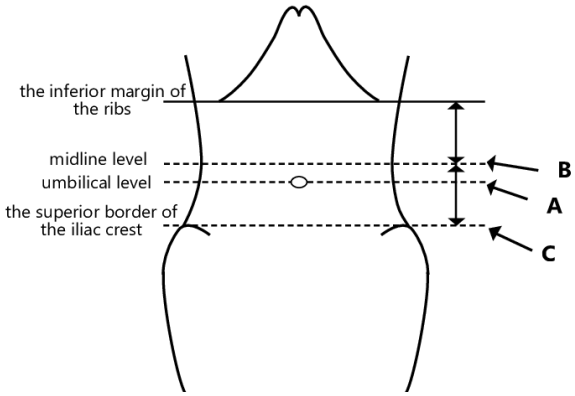

Fig. 5: Measurement of the size of the natural waist at the midline level. Note that the midline level (B) is not equal to their umbilical level (A) in all patients.

Neck circumference. When measuring the neck circumference, the chosen reference point was the upper edge of the thyroid cartilage (see Fig. 6). The patient was asked to be in an upright position with the head and chin at a normal 90° angle from the rest of the body (not looking up or down). The reference point was marked as shown in Fig. 6. A cloth metric ruler was used to measure neck circumference using a drawn reference point. The measurement was taken after the patient was asked to exhale.

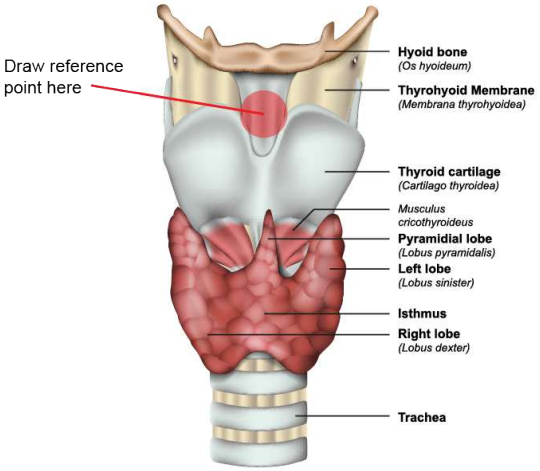

Fig. 6: Landmark used for measuring the neck circumference.

III. RESULTS

a) Histological evaluation of smooth-resurfacing protocols

Figure 7 shows the number of positive fibroblasts (*+F*) as measured using immuno-histochemical staining of histological samples with pro-collagen type I antibody at different skin depths 21 days following the treatment with three types of smooth-resurfacing protocols: Intense, Deep hyper-stacking and HyperStack™ (see Table 1 for the protocol parameters).

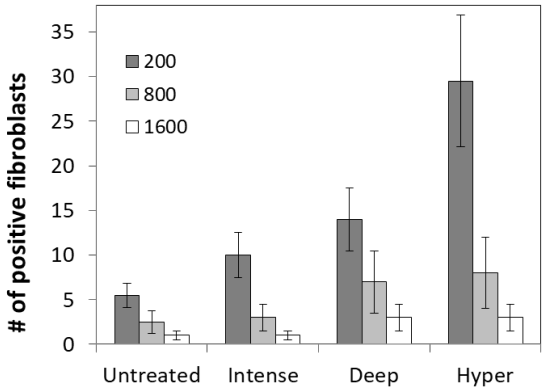

Fig. 7: Number of pro-collagen type I positive fibroblasts ($^{+}F_{21\,days}$) at tissue depths 200, 800 and 1600 μm at 21 days after the completed 4-session treatment using three types of smooth-resurfacing protocols presented in Table 1. Results for the untreated skin are also shown.

Similarly, Fig. 8 shows the gain (G) in the number of positive fibroblasts (^{+}F) depending on the skin depth and performed protocol, where the gain (G) is defined as

$$G = 100\%\ (\,{}^{+}F_{21\ days}/\,{}^{+}F_{untreated} - 1), \qquad (3)$$

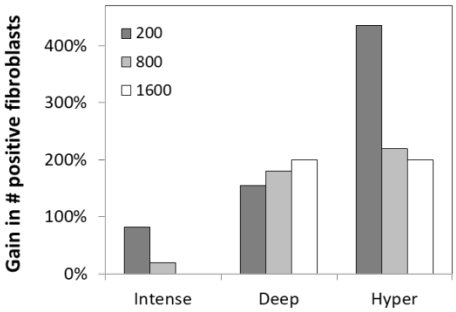

Fig. 8: Gain (G) in the number of pro-collagen type I positive fibroblasts at tissue depths of 200, 800 and 1600 μm at 21 days following the treatment with the Intense, Deep hyper-stacking and HyperStack™ protocols.

As can be seen from Figs. 7 and 8, all three protocols result in the enhanced pro-collagen expression. However, the combined effect of intense superficial triggering and deep coagulation as achieved using the HyperStack™ protocol results in the largest pro-collagen expression, extending at least up to 1600 μm deep within the skin.

b) Histological evaluation of the HyperStack™ protocol

Figures 9 and 10 depict the spatial distribution of the positive fibroblasts and the total number of fibroblasts, correspondingly, at 21 days and 3 months following the treatment with the HyperStack™ protocol. The graphs represent fibroblast values averaged over two separate abdominal skin samples taken from the same patient.

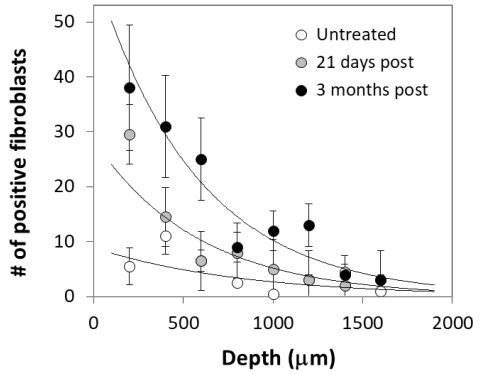

Fig. 9: Measured spatial distribution of pro-collagen type I positive fibroblasts for untreated skin, and at 21 days and 3 months following the HyperStack™ treatment. The lines are to guide the eye only.

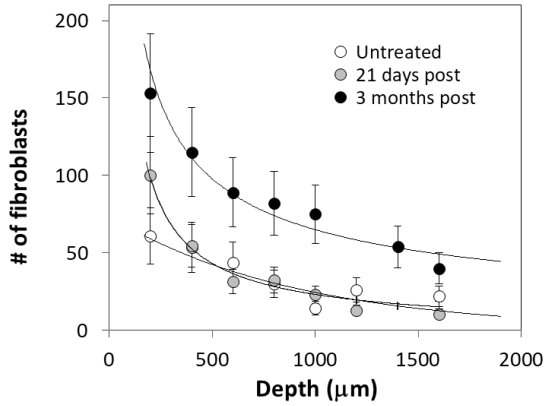

Fig. 10: Measured spatial distribution of all fibroblasts for untreated skin, and at 21 days and 3 months following the HyperStack™ treatment. The lines are to guide the eye only.

As can be seen from Fig. 11 below, the total number of positive fibroblasts located within the skin at depths up to 1600 μm doubled at the 21-day follow-up and increased by 4 times at the 3-month follow up.

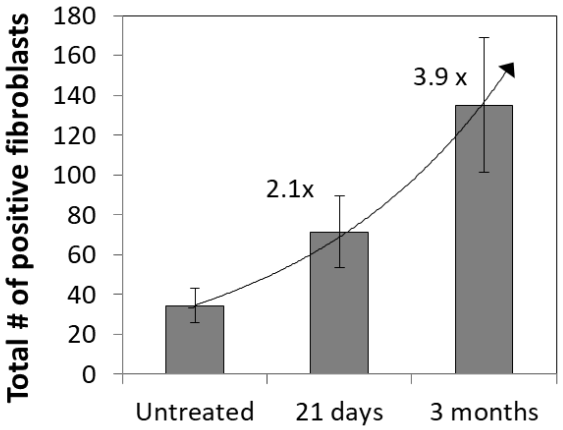

Fig. 11: Growth of the total number of positive fibroblasts located within the skin at depths up to 1600 μm at 21 days and 3 months following the HyperStack™ treatment.

On the other hand, the total amount of fibroblasts located within the skin at depths up to 1600 µm remained unchanged at 21 days following the HyperStack™ treatment, and then almost tripled at the 3-month follow up (Fig. 12).

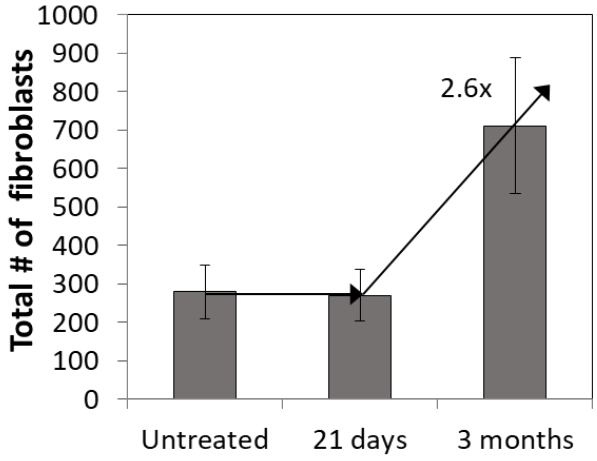

Fig. 12: Evolution of the number of all fibroblasts located within the skin at depths up to 1600 µm at 21 days and 3 months following the HyperStack™ treatment.

Histological samples of the HyperStack-treated patients showed improved thickness of the epidermis (acantosis), significant basal cells hyperplasia, increased number of papillae, and diffuse presence of white cells in the dermis with more compact collagen and elastin fibers (see Fig. 13). Also, the fibrilar component of the dermis appeared more organized and compact, with white cell infiltration (restorative reaction) and new vessel formation. The absence of perianexal adipose tissue was also observed (Fig. 13).

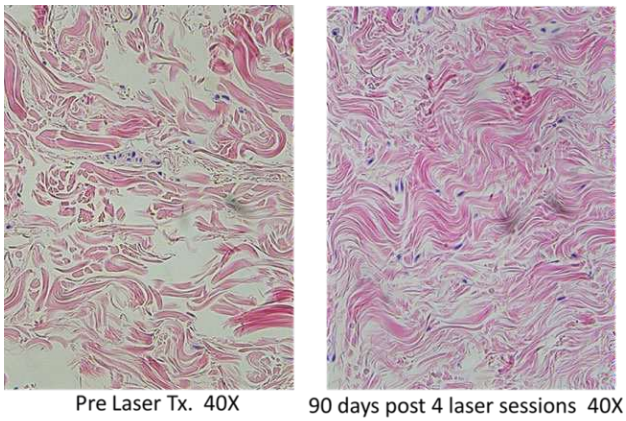

Fig. 13: Comparison of histological samples before and 90 days after four sessions of the HyperStack™ treatment. An increased number of fibroblasts can be observed. The fibrilar component of the dermis appears more organized, and new vessel formation can also be detected.

c) Clinical improvement

Clinical improvements following HyperStack™ treatment correlated with the histological results. A reduction of subcutaneous fat, superficial skin tightening and a reduction of sagging skin were observed post-treatment, resulting in an improved aesthetic appearance (Fig. 14).

Patients reported a feeling of warmth in the treated areas, and in some cases mild pain or discomfort. Post-treatment erythema lasted for few hours. No edema or other side effects were reported post treatment.

Fig 14: Clinical effect of the HyperStack™ treatment with T-Runner. Case 1: before, 30 and 150 days after four sessions (above from left to right) and before and Case 2: 90 days after 3 sessions (below from left to right). A reduction of subcutaneous fat, superficial skin tightening and a reduction in the waist circumference can be observed.

Although waist reduction was observed for all protocols, the superiority of the HyperStack™ protocol can also be concluded from Fig. 15, which shows the measured reduction in the waist circumference at 21 days, 3 months and 5 months following the treatment using different protocols. At 21 days the Intense protocol resulted in the largest reduction, however, it did not continue to improve at longer follow-ups. On the other hand, the HyperStack™ protocol caused the skin tightening process to continue for up to 5 months following the treatment, resulting in the largest final waist reduction.

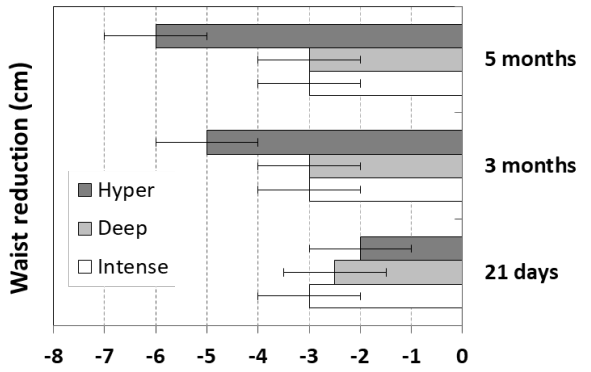

Fig. 15: Reduction in waist circumference at 21 days, 3 months and 5 months following 4-session treatments using the Intense, Deep hyper-stacking or HyperStack™ protocols.

Figure 16 shows an example of a treated neck of a male patient. The measured reduction in the neck's circumference was 1.5 cm after two sessions using the HyperStack™ protocol.

Fig. 16: Measurement of neck tightening following smooth-resurfacing. A reduction in the neck's circumference and superficial skin tightening was observed.

IV. DISCUSSION

The main goal of non-ablative "smooth-resurfacing" is to initiate remodeling of the sub-epithelial layer by activating the wound healing process in the skin. It has been shown that the healing response to thermal injury differs from the typical response after mechanical skin wounding (26). Thermal injury induces a rapid expression of heat-shock proteins that are regarded as key factors in the skin remodeling phase following laser treatment (26).

Collagen is the main structural protein in the extracellular matrix of the skin. In the healing wound, collagens are synthesized by cells such as fibroblasts and modified into complex morphologies. The type, amount and organization of collagen changes in the healing wound and determines the tensile strength of the healed skin. Collagen III is the first to be synthesized in the early stages of wound healing and is replaced by collagen I, the dominant skin collagen.

Fibroblasts play a crucial role in the production of collagen throughout the entire wound healing process following smooth-resurfacing treatment. In this study the activation of the healing process was measured by observing new collagen type I syntheses using immune-histochemical staining of pro-collagen type I fibroblasts (i.e., positive fibroblasts), and as well by measuring the total fibroblast count. The study shows that at early stages (21 days after the treatment) the collagen type I is produced mainly by the activation of existing fibroblasts. This can be seen from the increase in the number of positive fibroblasts (Fig. 11; 21 days) within the unchanged total number of fibroblasts (Fig. 12; 21 days). In the next stage an enhancement of the fibroblast proliferation occurs as well, resulting in a 2.6 x increase in the total number of fibroblasts (Fig. 12; 90 days). Altogether, after 90 days the number of positive fibroblasts was measured to increase by a factor of almost 4 (Fig. 11; 90 days), resulting in a further enhancement of the production of new collagen during the second stage.

The above findings are consistent with the results of a previously published study showing an elevation of procollagen I and III levels throughout the upper to mid dermis from 1 week to 3 months following Er:YAG laser smooth-resurfacing [10], and as well with previous studies on women with stress urinary incontinence (SUI) and genitourinary menopause syndrome (GMS), where increased fibroblast counts with signs of synthetic activity was observed at 2 months after smooth-resurfacing laser therapy [1].

The Er:YAG laser-generated heat dynamics during smooth-resurfacing exhibits a unique superficially intense heat-shock triggering phenomena, in addition to the conventional stimulation of fibroblasts through the gradual build-up of the spatial temperature distribution extending several hundred microns deep into the tissue. When the patient's pain tolerance is used as the treatment safety criteria for selecting appropriate laser parameters, this heat dynamics leads to three distinct treatment protocol regimens: i) Intense smooth-resurfacing for maximal superficial heat-shock triggering with relatively low coagulation depth; ii) Deep hyper-stacking smooth-resurfacing for maximal deep-thermal stimulation with low heat-shock triggering amplitude; iii) HyperStack™ smooth-resurfacing which combines the effects of superficial triggering and coagulation, resulting in medium heat-shock triggering amplitudes, A_{trig} and medium coagulation depths, z_t (See Table 1). In this study, the

HyperStack™ regimen was found to be the most effective considering the obtained histological and clinical results.

Relative effectiveness of smooth-resurfacing protocols. When comparing the effects of the three smooth-resurfacing protocols, one must also take into account the maximal treatment fluence (F_s) that can be delivered with each of the protocols without causing intolerable discomfort to the patient.

Measurements of the pain threshold have shown that the feeling of pain depends predominantly on the final skin temperature (T_s; see Fig. 1) that is reached at the end of the smooth-resurfacing laser pulse sequence, and not on the short high-temperature peaks ($T_{max\text{-}i}$). It has also been shown that the temperature increase $\Delta T_s = T_s - T_0$, above the initial skin temperature T_0 depends on the delivered fluence (F_s) and the treatment sequence duration (t_s) according to

$$\Delta T_s \approx A_s . F_s . t_s^{Ks}, \quad (4)$$

where for cutaneous tissues, $A_s = 84$ and $K_s = -0.43$. As can be concluded from Eq. 4, longer smooth-resurfacing sequences result in lower final skin temperatures, and therefore with longer sequences, higher fluences can be delivered for the same level of patient discomfort.

During the Intense protocol, the total fluence is delivered in a series of intense micro pulses. This means that the pain threshold temperature is reached after a smaller number of pulses, and therefore also within a shorter time, t_s. On the other hand, with the Deep protocol, the total fluence is delivered in a longer series consisting of a larger number of low-intensity micro pulses. Therefore, as compared to the Intense protocol, higher total fluences can be delivered with the Deep hyper-stacking protocol before exceeding the pain threshold temperature and the corresponding STP limit. This can also be seen from Table 1, where treatment fluences below the pain threshold are shown to be F_s = 4.2, 11 and 14 J/cm² for the Intense, HyperStack™ and Deep hyper-stacking treatment protocols, correspondingly. The HyperStack™ fluence is thus in between the values for the Intense and Deep protocols.

Therefore, in order to compare the actual effectiveness of the three protocols from a biochemical standpoint, the differences in the delivered fluences must be also taken into account. This can be done by considering the gain coefficient $g = G/F_s$, representing the gain in positive fibroblasts (see Eq. 3) normalized to the delivered fluence F_s. The resulting gain coefficients for the three protocols described in Table 1 are shown in Fig. 17.

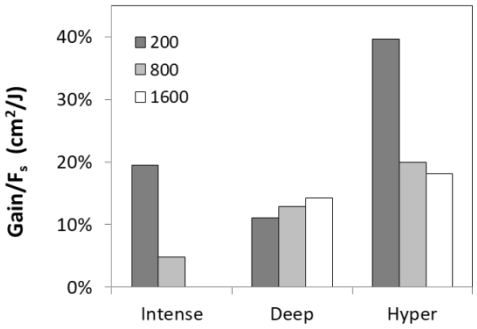

Fig. 17: Gain coefficient $g = G/F_s$, for the number of pro-collagen type I positive fibroblasts at tissue depths of 200, 800 and 1600 μm at 21 days following treatment with the Intense, Deep hyper-stacking and HyperStack™ protocols.

As can be concluded from Fig. 17, the Intense protocol characterized by high superficial heat-shock triggering amplitude (A_{trig}) results in a higher pro-collagen expression in the superficial skin layers, in comparison to the Deep hyper-stacking protocol that triggers the synthesis of collagen type I in deeper tissue layers by the mechanism of standard tissue coagulation. This finding is in agreement with the previously postulated superficial heat-shock triggering mechanism [2, 3, 22, 24]. The superficial heat shocking resembles the micro-needling technique, aimed at stimulating tissue renewal through triggering cell-to-cell communication and a wound-healing like response, without inducing epidermal injury through removal or ablation [31, 32]. The smooth-resurfacing laser-induced thermal triggering mechanism can thus be viewed as non-ablative thermal "needling" (i.e., triggering) of the total treated skin surface, with the action of the spatially sharp needles being replaced by the action of temporarily "sharp" but spatially extended heat-shock pulses.

With the HyperStack™ protocol, a combined effect of superficial triggering and deep coagulation can be observed resulting in the stimulation of collagen type I synthesis up to 1600 μm deep at the 3-month follow up (Figs. 9, 10 and 17). The effect of tissue regeneration extends deeper than the coagulation depths predicted by the numerical model (see Fig. 17 and Table 1). This observation is tentatively attributed to the additional heat-shock triggering mechanism that accompanies treatments with short-duration Er:YAG pulses.

Recommended HyperStack™ parameters. The most effective smooth-resurfacing protocol was found to be the HyperStack™ protocol, which is based on activating both the heat-shock triggering and the deep-

tissue coagulation mechanism. The model simulations and clinical results indicate that higher levels of superficial heat-shock triggering and deeper coagulation can be achieved when using parameters resulting in higher STP values. For STP values above the patient's discomfort tolerance, the use of topical anesthesia is recommended.

Tables 2 and 3 below show the recommended ranges of the HyperStack™ treatment parameters without (Table 2) or with (Table 3) topical anesthesia when using a full-beam T-Runner scanner with a Dynamis laser system. It is to be noted that these protocols should serve only as basic treatment guidelines. It is recommended that the operator selects the parameters depending on the individual patient's sensitivity to discomfort. Especially when exceeding the STP values of 100%, a small test area/spot treatment is recommended to be performed prior to the full-area treatment.

Table 2. Recommended range of HyperStack™ smooth-resurfacing parameters for the Fotona Dynamis laser devices equipped with the full-beam T-Runner robotic scanning handpiece. Four sessions performed without topical anesthesia (if tolerated by the patient) and separated by at least one week are recommended.

T-Runner Face w/o topical anesthesia		**HyperStack smooth-resurfacing**					
V-SMOOTH mode	ms	500	500	625	625	625	625
Fluence, F_s	J/cm²	5.4	6.6	6.0	7.2	6.3	9.0
N_{stack}	/	6	6	6	6	7	10
STP	%	98	120	99	119	97	119
Coagulation depth, z_c	µm	97	187	110	207	111	301
Heat shock trig., A_s	/	0.11	0.30	0.19	0.39	0.22	0.14

Table 3. Recommended range of HyperStack™ smooth-resurfacing parameters for the Fotona Dynamis laser devices equipped with the full-beam T-Runner robotic scanning handpiece. Four sessions performed using topical anesthesia and separated by at least one week are recommended.

T-Runner Body & Face w/o topical anesthesia		**HyperStack smooth-resurfacing**					
V-SMOOTH mode	ms	625	625	625	625	625	625
Fluence, F_s	J/cm²	9.6	9	9.6	10.8	11.7	11
N_{stack}	/	12	10	11	12	13	11
STP	%	117	119	126	132	138	140
Coagulation depth, (z_c)	µm	333	301	388	481	576	522
Heat shock triggering (A_{trig})	/	0.04	0.14	0.15	0.15	0.17	0.24

V. CONCLUSIONS

The results of this study are consistent with previous reports that smooth-resurfacing with Er:YAG laser possesses a unique, non-ablative regenerative characteristic, whereas the standard deep-thermal coagulation is accompanied and enhanced by an additional intense heat-shock biomodulation mechanism.

When comparing different smooth-resurfacing protocols, the obtained immuno-histological data indicates that the most effective protocol is the HyperStack™ protocol based on activating both the intense heat-shock biomodulation and the deep-tissue coagulation mechanisms.

The tissue regeneration process persists for more than 3 months following the HyperStack™ smooth-resurfacing, as can be seen from the total amount of positive fibroblasts located within skin depths of up to 1600 µm, which was shown to double at the 21-day follow up and to increase by 4-fold at the 3-month follow up (Fig. 11). The waist circumference was measured to decrease by 2 cm at 21 days, 5 cm at 3 months and 6 cm at 5 months following the HyperStack™ treatment of abdominal skin (Fig. 15).

Acknowledgments

This research was supported by the Ministry of Education, Science and Sport, Slovenia and the European Regional Development Fund (Project GOSTOP). The authors are affiliated also with Fotona, d.o.o.

REFERENCES

1. Hympanova L, Mackova K, El-Domyati M, Vodegel E, Roovers JP, Bosteels J, Krofta L, Deprest J (2020) Effects of non-ablative Er:YAG laser on the skin and the vaginal wall: systematic review of the clinical and experimental literature. Int Urogynecol J; https://doi.org/10.1007/s00192-020-04452-9
2. Lukac M, Zorman A, Bajd F (2018) TightSculpting®: A Complete Minimally Invasive Body Contouring Solution; Part II: Tightening with FotonaSmooth® Technology. J Laser Health Acad 2018; 2018(1); 26-35.
3. Lukac M, Gaspar A, Bajd F (2018) Dual Tissue Regeneration: Non-Ablative Resurfacing of Soft Tissues with FotonaSmooth® Mode Er:YAG Laser. J LA&HA, J Laser Health Acad 2018; 2018(1); 1-15.
4. Fistonic N, Fistonic I, Findri Gustek S, Sorta Bilajac Turina D, Franic D, Vizintin Z, Kazic M, Hreljac I, Perhavec T, Lukac M . Minimally invasive, non-ablative Er:YAG laser treatment of stress urinary incontinence in women – a pilot study. Lasers Med Sci 2016; 31: 635-643
5. Gaspar A, Brandi H (2017) Non-ablative erbium YAG laser for the treatment of type III stress urinary incontinence (intrinsic sphincter deficiency). Laser Med Sci 2017; Apr 32(3):685-691 (2017).

6. Vizintin Z, Lukac M, Kazic M, Tettamanti M. Erbium laser in gynecology, Climacteric 2015; 18(1): 4-8.
7. U.B. Ogrinc, S. Sencar, H. Lenasi (2015) Novel Minimally Invasive Laser Treatment of Urinary Incontinence in Women, Lasers Surg Med 2015;.Nov 47(9): 689–697.
8. Mitsuyuki M, Stok U, Hreljac I, Yoda K, Vizintin Z. Treating Vaginal Laxity Using Nonablative Er:YAG Laser: A Retrospective Case Series of Patients From 2.5 Years of Clinical Practice. Sex Med 2020 Feb; 1-9.
9. Mija Blaganje M, Šćepanović, Žgur L, Verdenik I, Franja Pajk F, Lukanović A. Non-ablative Er:YAG laser therapy effect on stress urinary incontinence related to quality of life and sexual function: A randomized controlled trial. Eur J Obstet Gynecol Reprod Biol 2018; 224:153-158.
10. Ebrahim HM, Gharib K (2018) Correction of nasolabial folds wrinkle using intraoral non-ablative Er:YAG laser, Journal of Cosmetic and Laser Therapy 2018; DOI:10.1080/14764172.2018.1439964: 1-5.
11. Quezada Gaón N, Binfa F. The effect of intraoral 2,940nm nonablative Erbium:YAG laser on the rejuvenation of the upper lip: a pilot study. Surg Cosmet Dermatol 2017;9(1):56-8.
12. Storchi IF, Parker S, Bovis F, Benedicenti S, Amaroli A. Outpatient erbium:YAG (2940 nm) laser treatment for snoring: a prospective study on 40 patients. Lasers Med Sci 2018, 33(2):399-406.
13. Shiffman H, Lukac M (2018) NightLase®: Minimally Invasive Laser-Assisted Uvulopalatoplasty. J LA&HA, J Laser Health Acad 2018; 2018(1); 39-44.
14. Neruntarat C, Khuancharee K, Shoowit P. Er:YAG laser for snoring: a systemic review and meta-analysis. Lasers Med Sci. 2020 Aug; 35(6):1231-1238.
15. Frelich H, Ścierski W, Marków M, Frelich J, Frelich H, Maciej M . Minimally invasive erbium laser treatment for selected snorers. Lasers Med Sci . 2019 Sep;34(7):1413-1420
16. Majaron B, Srinivas SM, Huang HL, Nelson JS. Deep coagulation of dermal collagen with repetitive Er:YAG laser irradiation. Lasers Surg. Med 2000; 26:215–222
17. Majaron B, Kelly KM, Park HB. Er:YAG Laser Skin Resurfacing Using Repetitive Long-Pulse Exposure and Cryogen Spray Cooling: I. Histological Study Lasers Surg Med 2001; 28:121-130.
18. Majaron B, Verkruysse W, Nelson S. Er:YAG Laser Skin Resurfacing Using Repetitive Long-Pulse Exposure and Cryogen Spray Cooling: II. Theoretical Analysis. Lasers Surg Med 2001; 28:131-137
19. Kunzi-Rapp K, Dierickx CC, Cambier B, Drosner M.(2006) Minimally invasive skin rejuvenation with Erbium: YAG laser used in thermal mode. Lasers Surg Med. 2006 Dec;38(10):899-907.
20. Drnovsek Olup B, Beltram M, Pizem J. Repetitive Er:YAG laser irradiation of human skin: A histological evaluation. Lasers Surg Med 2004; 35:146–151
21. Ross EV et al . Use of a novel Erbium laser in a Yucatan minipig: A study of residual thermal damage, ablation, and would healing as a function of pulse duration. Lasers Surg Med 2002; 30; 93-100.
22. Lukac M, Lozar A, Perhavec T, Bajd F. Variable heat shock response model for medical laser procedures, Lasers Med Sci. Aug 2019;34(6):1147-1158.
23. Majaron B, Plestenjak P, Lukac M .Thermo-mechanical laser ablation of soft biological tissue: modeling the micro-explosions. Appl. Phys. B 1999; 69, 71–80
24. Lukac M, Zorman A, Lukac N, Perhavec T, Tasic-Muc B. Characteristics of Non-Ablative Resurfacing of Soft Tissues by Repetitive Er:YAG Laser Pulse Irradiation. Lasers Surg Med 2021. Accepted for publication.
25. Bowman PD. Survival of human epidermal keratinocytes after short-duration high temperature: synthesis of HSP70 and IL-8. Am J Physiol 1997; 272(6 Pt 1):C1988-94.
26. Capon A, Mordon S. Can thermal lasers promote skin wound healing?. Am J Clin Dermatol 2003; 4 (1): 1-12
27. Mackanosa MA, Contag CH. Pulse duration determines levels of Hsp70 induction in tissues following laser irradiation. J Biomed Opt 2011; 16(7), 078002 (July 2011)
28. Lubart R, Friedmann H, Lavie R, Baruchin A . A novel explanation for the healing effect of the Er:YAG laser during skin rejuvenation. Journal of Cosmetic and Laser Therapy 2011; 13: 33–34
29. Manstein D, Scott Herron G, Kehl Sink R, Tanner H, Anderson R. Fractional Photothermolysis: A New Concept for Cutaneous Remodeling Using Microscopic Patterns of Thermal Injury. Lasers Surg Med 2004; 34:426–438.
30. Ganceviciene R et al. Skin anti-aging strategies. Dermatoendocrinol 2012; 4(3): 308–319.
31. Zhu H. Acupoints Initiate the Healing Process. Medical Acupuncture 2014; 26(5): 264-270
32. Horst Liebla, Luther C. Kloth. Skin Cell Proliferation Stimulated by Microneedles. Journal of the American College of Clinical Wound Specialists 2013; 4(1): 2–6.
33. Johnson FH, Eyring H, and Stover BJ. The Theory of Rate Processes in Biology and Medicine. Wiley 1974; New York.
34. Wright NT (2003) On a relationship between the Arrhenius parameters from thermal damage studies. J Biomech Eng 2003; 125(2):300–304.
35. Henriques FC, Moritz AR . Studies of thermal injury, 1. The conduction of heat to and through skin and the temperature attained therein. A theoretical and an experimental investigation. A J Pathol 1947; 23:531–549
36. Moritz AR, Henriques FC. Studies of thermal injury, 2. The relative importance of time and surface temperature in the causation of burns. A J Pathol 1947; 23:695–720.
37. Menendez AR, Cheney FE, Zuclich JA, Crump P. Probability-summation model of multiple laser-exposure effects. Health Phys 1993; 65:523–528.
38. Brian J. Lund, David J. Lund, and Peter R. Edsall. Damage threshold from large retinal size repetitive-pulse laser exposures. Health Physics 2014; 107(4):292-299
39. Griess, GA, Blankenstein MF, Williford GG. Ocular damage from multiple-pulse laser exposures. Health Physiscs 198;. 39 (Dec):921-927.